Bidirectional RO-ISAC Using Polarization Division Duplexing With a Polarization-Maintaining CCR

Shiyun He, Chen Chen, *Senior Member, IEEE*, Zhihong Zeng, *Member, IEEE*, Dengke Wang, Fengli Yang, Mingqing Liu, *Member, IEEE*, and Harald Haas, *Fellow, IEEE*

***Abstract*—Optical integrated sensing and communication has attracted extensive attention in sixth-generation (6G) networks, while retroreflective optical integrated sensing and communication (RO-ISAC) systems that adopt the corner cube reflector (CCR) to enhance optical reflection exhibit tremendous development potential. In this paper, a bidirectional RO-ISAC system based on polarization division duplexing (PDD) using a polarization-maintaining CCR (PM-CCR) is proposed and experimentally demonstrated. Specifically, the proposed bidirectional RO-ISAC system utilizes orthogonal polarizers to avoid the interference between the reflected downlink signal and uplink signal. Meanwhile, PM-CCR is employed to preserve the polarization state of the reflected downlink signal. To ensure the orthogonality of the polarization state at the downlink and uplink transmitters in real time and adapt to practical mobile scenarios, a polarization state tracking and control module is considered, which further enhances the stability of the system. Experimental results successfully verify the feasibility of the proposed bidirectional RO-ISAC system based on PDD and PM-CCR.**

***Index Terms*—Bidirectional transmission, corner cube reflector, polarization division duplexing, polarization maintaining, retroreflective optical integrated sensing and communication.**

I. Introduction

THE rapid development of sixth-generation (6G) communication technologies imposes a demand on communication systems to possess the sensing capability of communication targets while ensuring high reliability and high data rates, which can effectively improve spectral efficiency and endow the systems with multi-dimensional information support [1]. Integrated sensing and communication (ISAC) systems are able to effectively balance the two core functions of communication and sensing. At present, the academic community has conducted extensive research on radio frequency (RF) ISAC systems [2]; however, constrained by limited spectral resources, it is difficult to further enhance their communication and sensing performance. In contrast, optical wireless ISAC systems based on lightwaves (including infrared, visible, and ultraviolet bands) have wider spectral resources and higher sensing accuracy, thus exhibiting greater development potential than their RF counterparts [3], [4]. Meanwhile, the newly proposed retroreflective optical ISAC (RO-ISAC) system in recent years has greatly improved the reflection intensity of optical signals by deploying a corner cube reflector (CCR) at the target side [5], [6]. Compared with traditional optical ISAC systems that rely on active sensing, the RO-ISAC system achieves high-efficiency passive sensing, which neither occupies the sensing modulation bandwidth nor introduces additional implementation complexity to the target side [7], [8].

In the RO-ISAC system, waveform design plays a pivotal role in achieving high-performance communication and sensing. At present, the academic community has proposed a variety of waveform schemes tailored to ISAC requirements, such as pulse sequence sensing and pulse position modulation (PSS-PPM) [9], combined linear frequency modulation and continuous phase modulation (LFM-CPM) [10], pulse amplitude modulation (PAM)-based waveform [11], and orthogonal frequency division multiplexing (OFDM) [12]. Among these, OFDM technology is recognized as a preferred waveform candidate for the RO-ISAC system [13], owing to its synergistic advantages of high-rate transmission capability and superior sensing adaptability. Moreover, in the bidirectional transmission of RO-ISAC systems, mutual interference might exist between the downlink signal reflected by the CCR and the uplink signal, and how to avoid bidirectional interference remains a noteworthy research issue. In our previous work, a bidirectional interference cancellation scheme based on time division duplexing (TDD) has been proposed; however, TDD only enables half-duplex transmission and cannot realize full-duplex transmission [14]. In addition, another bidirectional interference cancellation scheme based on wavelength division duplexing (WDD) has been also proposed, yet duplex transmission with WDD precludes the implementation of wavelength division multiplexing (WDM), thus reducing the capacity of the system [15].

Received 8 May 2026; revised 29 June 2026; accepted 23 July 2026. Date of publication 27 July 2026; date of current version 16 September 2026. This work was supported in part by the National Natural Science Foundation of China under Grant 62271091 and Grant 62501088 and in part by the Open Research Fund of National Mobile Communications Research Laboratory, Southeast University under Grant 2026D08. *(Corresponding author: Zhihong Zeng.)*

Shiyun He, Chen Chen, Dengke Wang, and Fengli Yang are with the School of Microelectronics and Communication Engineering, Chongqing University, Chongqing 400044, China (e-mail: 202412021101t@stu.cqu.edu.cn; c.chen@cqu.edu.cn; dengke.wang@cqu.edu.cn; cqu_yfl@cqu.edu.cn).

Zhihong Zeng is with the School of Microelectronics and Communication Engineering, Chongqing University, Chongqing 400044, China, and also with National Mobile Communications Research Laboratory, Southeast University, Nanjing 210096, China (e-mail: zhihong.zeng@cqu.edu.cn).

Mingqing Liu is with the College of Electronics and Information Engineering, Tongji University, Shanghai 200092, China (e-mail: clare@tongji.edu.cn).

Harald Haas is with the Department of Engineering, Electrical Engineering Division, Cambridge University, CB3 0FA Cambridge, U.K. (e-mail: huh21@cam.ac.uk).

Color versions of one or more figures in this article are available at https://doi.org/10.1109/JLT.2026.3717052.

Digital Object Identifier 10.1109/JLT.2026.3717052

TABLE I
COMPARISON OF THE PROPOSED PDD SCHEME WITH OTHER BIDIRECTIONAL TRANSMISSION SCHEMES

Reference	Scheme	Duplexing mode	Pros	Cons
[14]	TDD	Half	One wavelength, channel symmetry	Halved capacity, bidirectional synchronization
[15]	WDD	Full	High capacity	Two wavelengths, channel asymmetry
This work	PDD	Full	One wavelength, channel symmetry, high capacity	Polarization maintaining

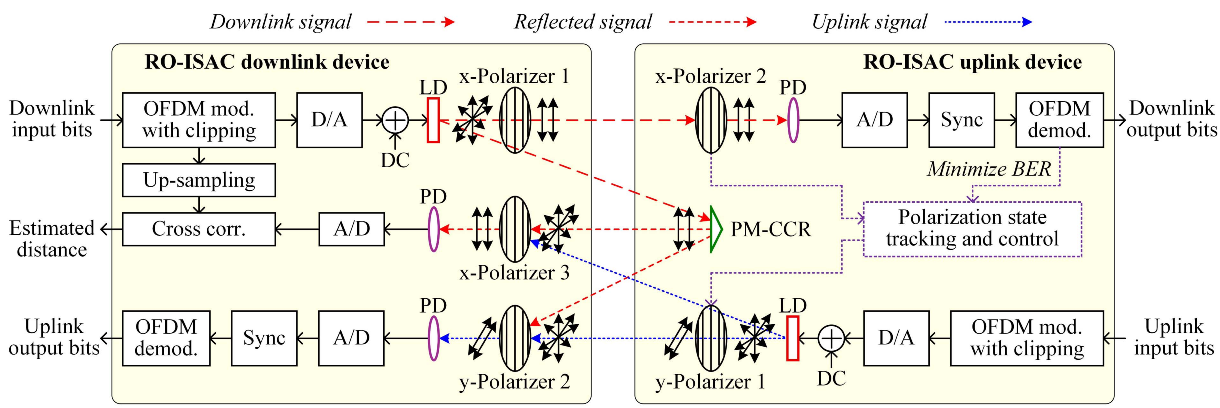

Fig. 1. Schematic diagram of the proposed bidirectional RO-ISAC system using PDD and PM-CCR. mod.: modulation; demod.: demodulation; corr.: correlation.

As a transverse wave, light is characterized by an electric field that oscillates perpendicular to its propagation direction. For this reason, two orthogonal and non-interfering polarization states can be employed as independent transmission channels for data transmission via polarization multiplexing (PolM) [16]. Therefore, this paper proposes a bidirectional RO-ISAC system based on polarization division duplexing (PDD) with a polarization-maintaining CCR (PM-CCR). The polarization characteristics of visible light provide a new degree of freedom for the improvement of system performance, and the elimination of bidirectional interference via PDD allows the release and integration of schemes such as WDM, thereby effectively enhancing the system capacity. This system mitigates bidirectional interference by virtue of PDD, adopts a PM-CCR to preserve the polarization state of reflected signals, and a polarization state tracking and control module is further proposed to refine the system. Proof-of-concept experiments are conducted to verify the feasibility of the proposed bidirectional RO-ISAC system based on PDD and PM-CCR. Table I compares the proposed PDD scheme with other bidirectional transmission schemes. For TDD, it can only support half-duplex transmission with halved capacity which requires strict bidirectional synchronization. For WDD, it achieves high capacity but suffers from channel asymmetry due to the use of two distinctive wavelengths. In contrast, PDD enjoys both high capacity and channel symmetry with a single wavelength but requires polarization maintaining.

II. PRINCIPLE

A. System Model

Fig. 1 illustrates the schematic diagram of the proposed bidirectional RO-ISAC system using PDD and PM-CCR, which consists of a downlink device and an uplink device. In the downlink device, the downlink input bits are first subjected to clipped OFDM modulation to reduce the peak-to-average power ratio (PAPR) [14]. Subsequently, the resultant digital OFDM signal is converted into an analog OFDM signal via digital-to-analog (D/A) conversion, with a direct current (DC) bias added to ensure the real-valued non-negativity of the signal. The obtained OFDM signal is then used to drive the laser diode (LD), which carries the downlink signal. In the uplink device, the optical signal is captured and converted into an electrical signal by a photodetector (PD). Analog-to-digital (A/D) conversion is subsequently performed to yield a digital OFDM signal, which undergoes synchronization before being fed into an OFDM demodulator to retrieve the output bits of the downlink signal. The demodulated data is input into a polarization state tracking and control module, which enables the estimation of the polarization state at the downlink receiver and the control of the polarization state at the uplink transmitter. As we can see, PM-CCR is employed in the uplink device of this system to reflect downlink signals, which enables the implementation of the cross-correlation ranging function in the downlink device of the system. In addition, the uplink signal is generated via the same procedure as the downlink signal and propagates through free space to the downlink device. Thus, the PDs in the downlink device capture the mixed light of the reflected downlink signal and the uplink signal, giving rise to non-negligible interference. To avoid interference between the reflected downlink signal and the uplink signal, a PDD-based interference cancellation scheme is proposed, which will be described in detail in the next subsection.

For the ranging process, when the PD captures the downlink signal reflected by the PM-CCR, A/D conversion is first performed. Subsequently, time-domain cross-correlation is conducted between the reflected downlink signal and the upsampled downlink signal to calculate the time of flight (ToF), thereby estimating the distance. The maximum likelihood estimation (MLE) of the ToF can be represented by $\hat{t} = \arg\max_t \sum_{n=0}^{W-1} y(n)x(n-t)$, where $x(n)$ and $y(n)$ respectively denote the upsampled time-domain samples of the downlink OFDM signal and the reflected time-domain samples of the downlink signal, and W is the window length for cross-correlation [5]. The ranging distance is obtained by $\hat{d} = c\hat{t}/2$, with c being the speed of light. For A/D sampling rate f_s, the ranging resolution is provided by $\Delta d = c/(2f_s)$.

B. PDD-Based Bidirectional Transmission

In bidirectional RO-ISAC systems, interference might exist between the reflected downlink signal and the uplink signal. To effectively avoid interference and enable bidirectional transmission, a PDD-based interference cancellation scheme is proposed for bidirectional RO-ISAC systems. In the downlink device of the RO-ISAC system, an x-direction polarizer (x-Polarizer 1) is placed in front of the LD, converting the downlink light into x-direction linearly polarized light. In the uplink device, a y-direction polarizer (y-Polarizer 2) is placed in front of the LD, converting the uplink light into y-direction linearly polarized light. Meanwhile, in the downlink device, an x-direction polarizer (x-Polarizer 3) is placed in front of the PD for the ranging module, which captures the reflected downlink light and rejects the y-direction uplink light. A y-direction polarizer (y-Polarizer 1) is placed in front of the PD for the uplink communication module, which receives the uplink light and shields the x-direction reflected downlink light. In the uplink device, an x-direction polarizer (x-Polarizer 2) is placed in front of the PD for receiving the downlink signal. If the x and y directions are perpendicular to each other, the downlink and uplink signals have orthogonal polarization states, which can avoid interference to a great extent.

For the bidirectional interference cancellation process, a polarization state tracking and control module is deployed to ensure the randomness of the polarization angle for bidirectional communication. In practical mobile scenarios, the polarization state of the downlink signal transmitter is generally unknown. In this paper, the polarization state of the downlink signal transmitter is randomly set to an unknown angle. The bit error rate (BER) is measured at different offset angles at the receiver, and the minimum BER is identified, which corresponds to the case where the polarization states of the transmitter and receiver are matched. By identifying this extreme point, the polarization state of the downlink transmitter can be estimated. At this point, setting the polarization state of the uplink transmitter to be orthogonal to that of the downlink transmitter enables polarization state tracking and control, thus avoiding interference in bidirectional transmission.

In practical RO-ISAC scenarios, platform vibration, atmospheric turbulence, and random rotation of retro-reflective terminals continuously distort the optical polarization state, resulting in time-varying inter-polarization crosstalk. The adopted polarization state tracking and control module adaptively compensates such dynamic polarization fluctuations to maintain stable duplex isolation. In terms of tracking speed, the closed-loop polarization state tracking and control scheme can rapidly capture polarization variations and complete microsecond-level compensation, effectively tracking fast channel fluctuations caused by turbulence and terminal jitter. In terms of robustness, real-time polarization calibration stabilizes the extinction ratio of orthogonal channels and suppresses dynamic self-interference, improving the system's environmental adaptability under time-varying channel conditions. In terms of latency, the digital-domain tracking mechanism introduces negligible extra delay, preserving the low-latency and continuous full-duplex characteristics of the PDD-based RO-ISAC system. Therefore, the polarization state tracking and control module ensures reliable integrated sensing and communication performance for PDD-based RO-ISAC systems in practical dynamic mobility scenarios.

As shown in Fig. 2, compared with the conventional CCR, the polarization ellipses of the output light from the PM-CCR are almost collinear with those of the input light for both horizontally and vertically polarized inputs. Therefore, the PM-CCR reflector can reduce the polarization state variation of the signal caused by reflection and better preserve the polarization state of the signal during transmission. This might be because the conventional CCR relies on total internal reflection (TIR), where the polarization state of the light changes when the reflected light passes through the conventional CCR. In contrast, the PM-CCR is coated with a metal film on its back surface and relies on specular reflection. Specular reflection occurs at the interface between glass and a metal with a higher refractive index, while TIR requires the backside medium (e.g., air) to have a lower refractive index. Compared with TIR, specular reflection can better preserve the polarization ellipticity of the input light beam.

Based on the above discussions, the key difference between the proposed PDD scheme and the general PolM scheme can be summarized as follows. More specifically, PolM uses two orthogonal polarization states for parallel data transmission in an unidirectional optical wireless communication (OWC) system to enhance system capacity [16], while PDD employs two orthogonal polarization states for downlink and uplink transmissions in a bidirectional RO-ISAC system to eliminate bidirectional interference. Moreover, although using modulating retro-reflector (MRR) can enable bidirectional transmission without bidirectional interference [17], the achievable uplink data rate is significantly limited by the low bandwidth of the MRR.

III. Experimental Results

Fig. 3 depicts the experimental setup of the bidirectional RO-ISAC system employing commercial optical transmitter and receiver modules. Clipped OFDM signals for the downlink and uplink are both generated offline via MATLAB and then uploaded to a two-channel arbitrary waveform generator (AWG, Tektronix AFG31102), with a sampling rate of 250 MSa/s for each channel. The peak-to-peak voltage (Vpp) of signals is 200 mV. The output signals of the AWG are combined with a 2.5 V DC bias voltage through a bias tee (Bias-T, Mini-Circuits

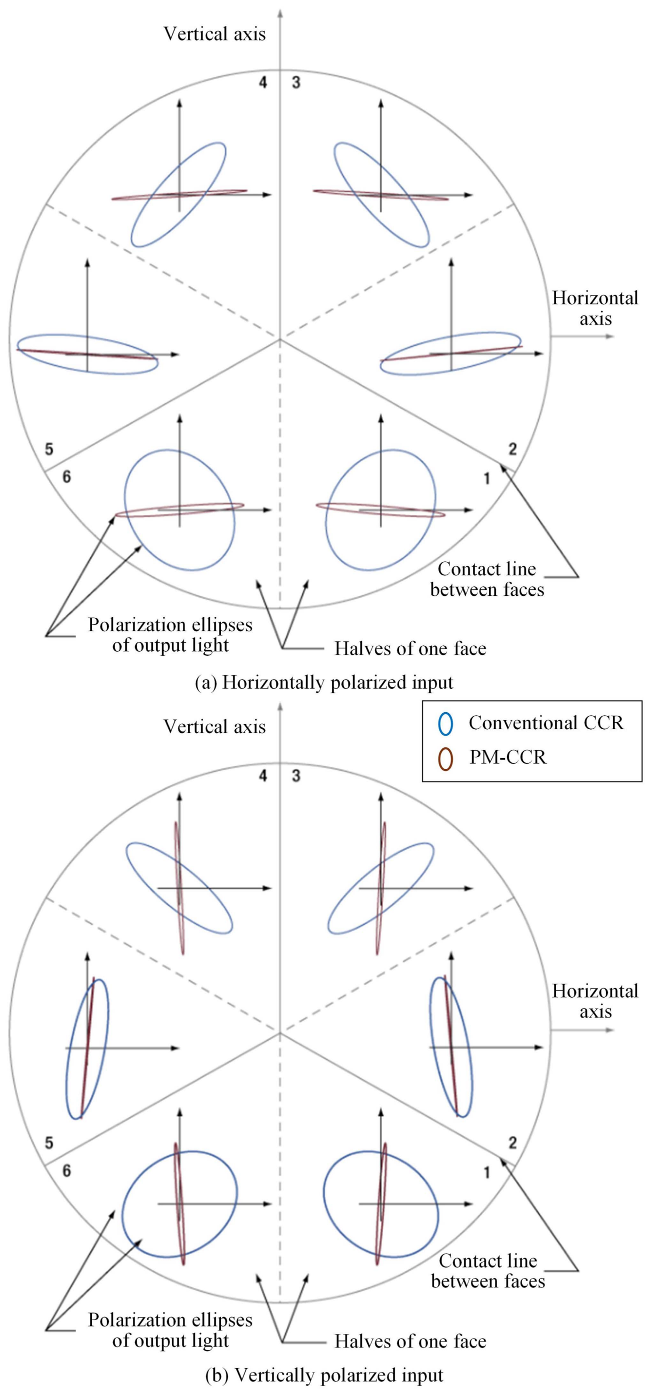

Fig. 2. Output polarization ellipse distributions of conventional CCR and PM-CCR under (a) horizontally polarized input and (b) vertically polarized input.

ZFBT-6GW+), which are then respectively used to drive two LD transmitters (HL63603TG) for x-Polarization downlink and y-Polarization uplink transmissions. In the downlink, an avalanche photo-diodes (APD, Hamamatsu C12702-12) is employed to capture the downlink signal. The acquired OFDM signal is recorded by a digital storage oscilloscope (DSO, Tektronix MDO32) at a sampling rate of 2.5 GSa/s for downlink demodulation. In the downlink device, an x-direction polarizer and a y-direction polarizer are adopted to filter the mixed optical signal

TABLE II
EXPERIMENTAL PARAMETERS

Parameter	Value
AWG sampling rate	250 MSa/s
DSO sampling rate	2.5 GSa/s
DC bias voltage	2.5 V
Vpp	200 mV
IFFT/FFT size	256
Number of data subcarriers	64
Constellation	BPSK
Clipping ratio	11 dB
Up-sampling ratio	10
Ranging resolution	6 cm
Distance	42-96 cm

(consisting of the uplink signal and the reflected downlink signal) in different polarization directions, and the filtered optical signals are detected by the APD separately. Specifically, the x-direction polarizer of the ranging module blocks the uplink signal, and the captured reflected downlink signal is recorded by the DSO at a sampling rate of 2.5 GSa/s for ranging; the y-direction polarizer of the uplink communication blocks the reflected downlink signal, and the captured uplink signal is recorded by the DSO at the same sampling rate for uplink demodulation. In the actual experiments, when the polarization state is set as a variable to be adjusted, the polarization state is altered by rotating the x/y polarizer for the convenience of measurement and data collection, thus enabling the acquisition of signal received by the APD at different rotation angles.

During OFDM modulation and demodulation, the size of inverse fast Fourier transform/fast Fourier transform (IFFT/FFT) is 256, the number of data subcarriers is 64, the constellation is binary phase shift keying (BPSK), and the clipping ratio is 11 dB. The transmission distance is set from 42 to 96 cm in the experiments. During time-domain cross-correlation based ranging, the up-sampling ratio is 10 and the ranging resolution is 6 cm. The detailed experimental parameters are listed in Table II. In our experiments, the transmission distance is limited within 1 m, which is mainly because of the low transmitted optical power and the bandwidth limitation of the adopted LD transmitters. By using LD transmitters with a higher transmitted optical power and a larger modulation bandwidth, meter-level or longer-distance transmission can be achieved. Moreover, beam divergence, detector sensitivity and polarization loss are also important factors limiting the feasible transmission distance, which can be jointly considered to ensure a satisfactory transmission distance for the bidirectional RO-ISAC system.

Fig. 4 depicts the relationship between the downlink communication BER and transmission distance for different rotation angles, with the polarization state of the downlink transmitter as the reference, under the condition that the transmitter's polarization state is known. It can be observed that for all rotation angles, the downlink BER increases with the increase in transmission distance, since the received signal power decreases as the distance becomes larger. In addition, at a given transmission distance, the polarization states of the transmitter and receiver are matched for a rotation angle of 0°, which allows linearly polarized light to transmit to the receiving PD without

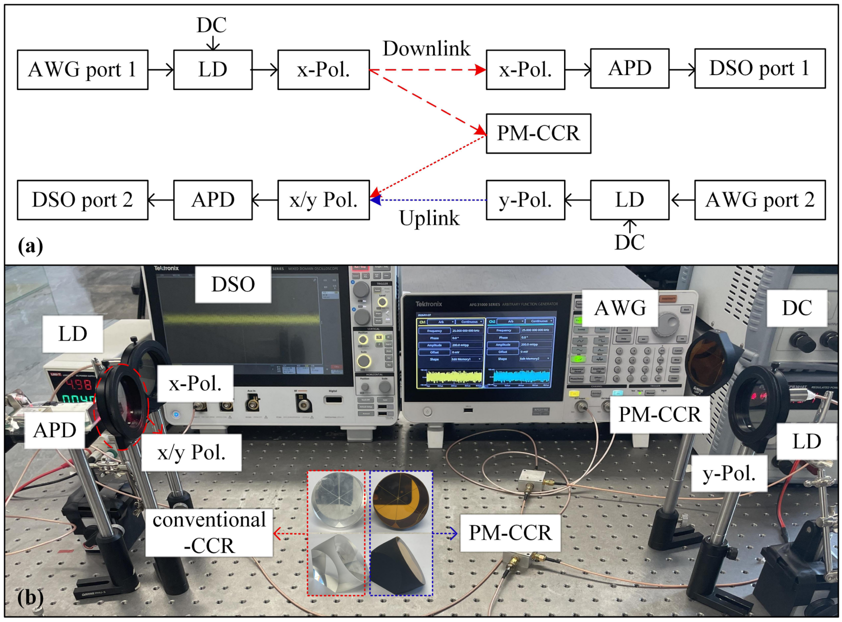

Fig. 3. Experimental setup of the bidirectional RO-ISAC system. Insets: (a) diagram of experimental testbed and (b) photo of experimental testbed.

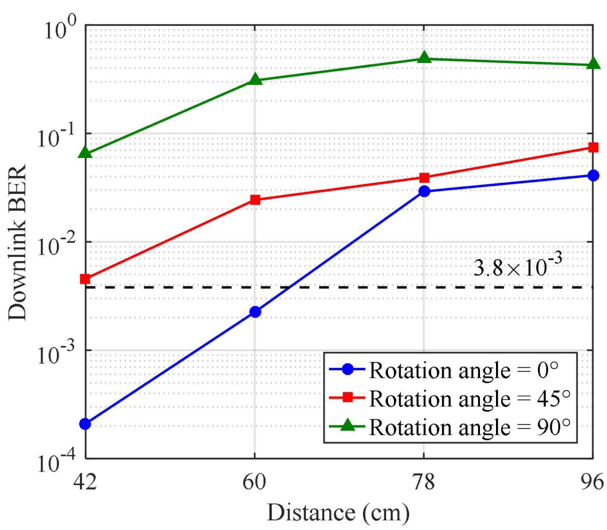

Fig. 4. Downlink BER vs. distance for different rotation angles.

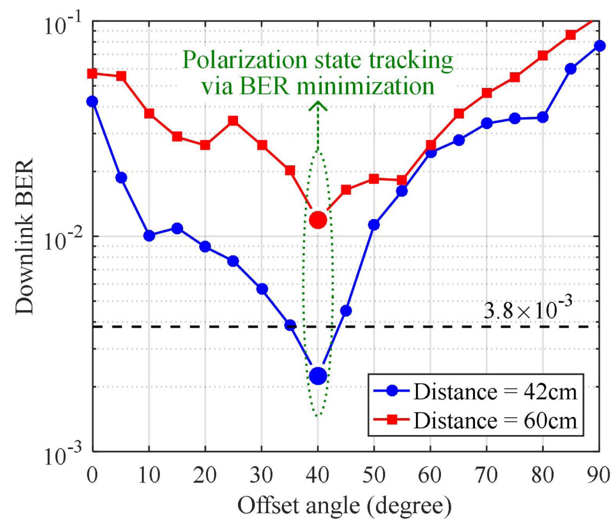

Fig. 5. Downlink BER vs. offset angle for polarization state tracking.

obstruction, resulting in the minimum BER. A rotation angle of 90°, meaning the polarization states of the transmitter and receiver are orthogonal, causes the linearly polarized light to be blocked by the orthogonal polarizer; consequently, the receiving PD cannot effectively capture the transmitted linearly polarized light, leading to the maximum BER. A rotation angle of 45° yields a BER performance that falls between these two extreme cases.

Fig. 5 depicts the relationship between the downlink BER and the offset angle at the transmission distances of 42 cm and 60 cm. In the polarization state tracking module, the polarization state of the downlink transmitter is unknown (set to 40° in the experiment). The polarization angle of the receiver is adjusted from 0° to 90° with a step size of 5°, and the downlink BER is measured accordingly. The results show that the BER first decreases and then increases in both cases, with a BER minimum observed at 40°; thus, the polarization state of the downlink transmitter is estimated to be 40°. Since orthogonal polarization states are required for the downlink and uplink, the polarization state of the uplink transmitter is adjusted to 130°.

Fig. 6 compares the relationship between the received signal-to-noise ratio (SNR) and the rotation angle for the downlink signals reflected by PM-CCR and conventional CCR. As the rotation angle increases from 0° to 90° with a step size of 15°, the received SNR of the signals reflected by both CCRs decreases. Specifically, the SNR of the PM-CCR decreases by 28.7 dB, while that of the conventional CCR only decreases by 9.7dB, corresponding to an approximate difference of 19 dB.

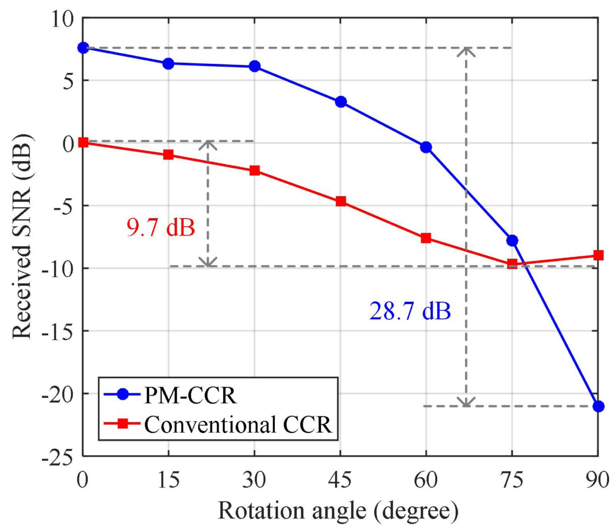

Fig. 6. Received SNR vs. rotation angle for PM-CCR and conventional CCR.

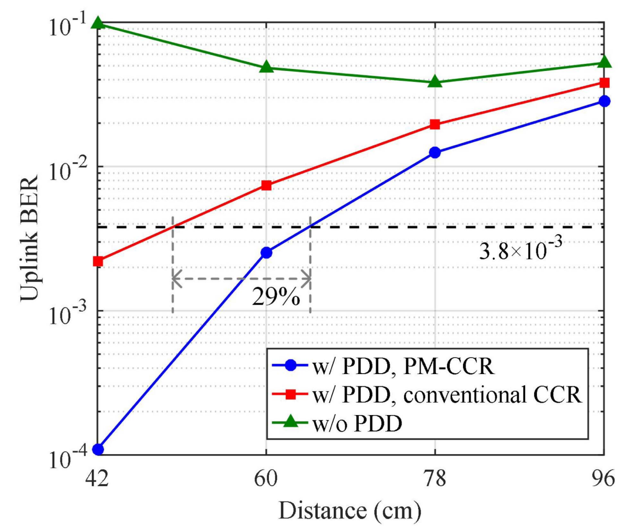

Fig. 7. Uplink BER vs. distance for two CCRs with and without PDD.

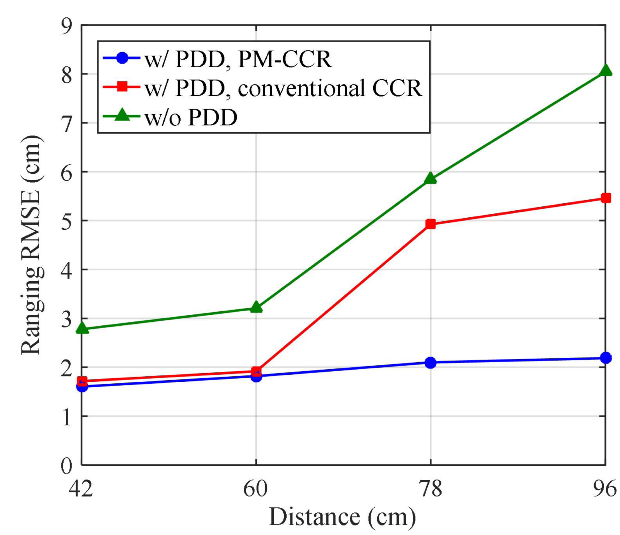

Fig. 8. Ranging RMSE vs. distance for two CCRs with and without PDD.

Furthermore, the received SNR of the PM-CCR is consistently higher than that of the conventional CCR when the rotation angle is not 90° (the polarization states of the transmitter and receiver are not completely orthogonal). At a rotation angle of 0°, most of the signal should ideally reach the PD; however, a portion of the signal reflected by the conventional CCR undergoes polarization state variation, and the altered signal cannot pass through the polarizer to reach the PD, resulting in a lower received SNR for the conventional CCR reflection link compared with the PM-CCR one. At a rotation angle of 90°, the signal should ideally be unable to pass through the polarizer to reach the receiving PD; nevertheless, a portion of the signal experiences polarization state variation, and the altered part of the signal can reach the PD, leading to a higher received SNR for the conventional CCR reflection link than the PM-CCR one. This indicates that reflection via the PM-CCR better preserves the polarization state of linearly polarized light, whereas reflection through the conventional CCR disturbs the polarization state of such light. Therefore, reflecting linearly polarized light with the PM-CCR can effectively maintain the polarization state of the reflected signal, enabling the signals that should pass through the polarizer to transmit more efficiently and those that should be blocked to be isolated more thoroughly.

Fig. 7 depicts the uplink communication performance, presenting the relationship between the uplink communication BER and transmission distance for different CCRs and in the absence of PDD. It can be observed that the adoption of PDD enables the elimination of bidirectional interference and a significant improvement in uplink BER performance; additionally, the PM-CCR outperforms the conventional CCR in terms of performance improvement, which is attributed to the better blocking effect of the PM-CCR on orthogonally polarized signals as elaborated earlier. Notably, in the absence of PDD, the uplink BER first decreases and then increases as the distance increases from 42 cm to 96 cm. This might be due to the fact that the attenuation of the reflected link is faster than that of the uplink signal in the distance range of 42 cm to 78 cm, where the reduction in interference plays a dominant role. More specifically, at the 7% forward error correction (FEC) coding limit of 3.8×10^{-3}, a distance extension of 29% can be achieved by using PM-CCR than using conventional CCR.

Fig. 8 depicts the relationship between the ranging root mean square error (RMSE) and transmission distance for different CCRs and in the absence of PDD. The RMSE increases with the increase in transmission distance in all cases, among which the RMSE is the largest in the absence of PDD and the smallest when the PM-CCR is employed. Compared with the case using conventional CCR, the RMSE is much lower for the case using PM-CCR when the distance is relatively long. More specifically, at a distance of 78 cm, the RMSE values are about 2, 5 and 6 cm for the cases without PDD, with PDD using conventional CCR and with PDD using PM-CCR, respectively. Fig. 9 depicts the ranging cross-correlation performance at a distance of 78 cm for different CCRs and in the absence of PDD. It can be seen that for a given cross-correlation window length W, the peak value of the

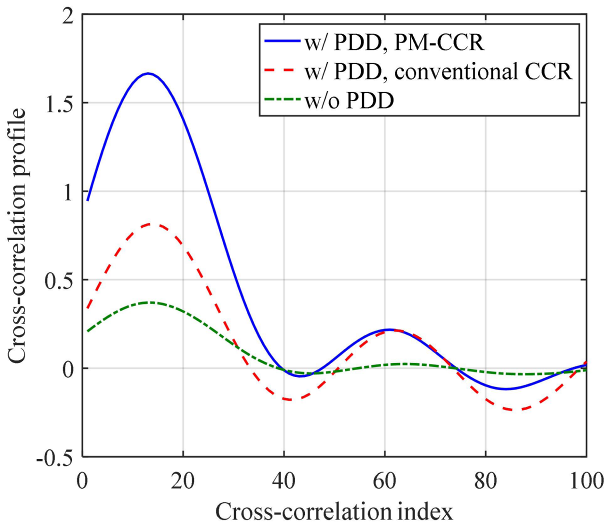

Fig. 9. Cross-correlation curves of two CCRs at a distance of 78 cm with and without PDD.

cross-correlation curve for the PM-CCR is higher than that for the conventional CCR, which demonstrates the superior cross-correlation performance of the PM-CCR. The cross-correlation performance with PDD is superior to that without PDD in all cases, which indicates that PDD can effectively eliminate uplink interference and improve the ranging performance.

IV. Conclusion

In this paper, we have proposed and experimentally demonstrated a bidirectional RO-ISAC system using PDD and PM-CCR. To avoid the interference between the reflected downlink signal and the uplink signal, a PDD-based interference cancellation scheme has been proposed, which utilizes orthogonal polarizers to enable bidirectional transmission. To achieve flexible adjustment of orthogonal polarization states in the bidirectional RO-ISAC system, a polarization state tracking and control module has been added to detect and control the orthogonality of the polarization states at the uplink device, thus enhancing the system stability. Meanwhile, comparative experiments have been conducted using the PM-CCR and the conventional CCR, which verify the performance advantage of the PM-CCR in preserving the polarization state of linearly polarized light. The experimental results successfully verify the feasibility of the bidirectional RO-ISAC system using PDD and PM-CCR. Considering that the use of PDD might suffer from the adverse effect of depolarization in scattering or turbulent channels, it is feasible to apply circularly polarized light instead of linearly polarized light for efficient mitigation of depolarization in PDD-based bidirectional RO-ISAC systems.

References

[1] C.-X. Wang et al., “On the road to 6G: Visions, requirements, key technologies, and testbeds,” *IEEE Commun. Surveys Tuts.*, vol. 25, no. 2, pp. 905–974, Second Quarter 2023.
[2] N. González-Prelcic et al., “The integrated sensing and communication revolution for 6G: Vision, techniques, and applications,” *Proc. IEEE*, vol. 112, no. 7, pp. 676–723, Jul. 2024.
[3] C. Liang et al., “Integrated sensing, lighting and communication based on visible light communication: A review,” *Digit. Signal Process.*, vol. 145, 2023, Art. no. 104340.
[4] Y. Wen, F. Yang, J. Song, and Z. Han, “Optical integrated sensing and communication: Architectures, potentials and challenges,” *IEEE Internet Things Mag.*, vol. 7, no. 4, pp. 68–74, Jul. 2024.
[5] Y. Cui et al., “Retroreflective optical ISAC using OFDM: Channel modeling and performance analysis,” *Opt. Lett.*, vol. 49, no. 15, pp. 4214–4217, 2024.
[6] T. Chu et al., “Retroreflective optical ISAC for 6G: Technologies, applications and future directions,” 2025, *arXiv:2512.01275*.
[7] H. Wang, Z. Zeng, C. Chen, B. Zhu, S. Shao, and M. Liu, “Retroreflective optical ISAC supporting 3D positioning in indoor environments,” in *Proc. Asia Commun. Photon. Conf.*, 2024, pp. 1–5.
[8] T. Chu et al., “Revolutionizing 6G: Experimental validation of an optical integrated communication, sensing, and power transfer system,” *IEEE J. Sel. Areas Commun.*, vol. 44, pp. 689–701, 2026.
[9] Y. Wen, F. Yang, J. Song, and Z. Han, “Pulse sequence sensing and pulse position modulation for optical integrated sensing and communication,” *IEEE Commun. Lett.*, vol. 27, no. 6, pp. 1525–1529, Jun. 2023.
[10] Y. Wen, F. Yang, J. Song, and Z. Han, “Free space optical integrated sensing and communication based on LFM and CPM,” *IEEE Commun. Lett.*, vol. 28, no. 1, pp. 43–47, Jan. 2024.
[11] J. Wang, N. Huang, C. Gong, W. Wang, and X. Li, “PAM waveForm design for joint communication and sensing based on visible light,” *IEEE Internet Things J.*, vol. 11, no. 11, pp. 20731–20742, Jun. 2024.
[12] E. B. Muller, V. N. Silva, P. P. Monteiro, and M. C. R. Medeiros, “Joint optical wireless communication and localization using OFDM,” *IEEE Photon. Technol. Lett.*, vol. 34, no. 14, pp. 757–760, Jul. 2022.
[13] Y. Wen, F. Yang, J. Song, and Z. Han, “Free space optical integrated sensing and communication based on DCO-OFDM: Performance metrics and resource allocation,” *IEEE Internet Things J.*, vol. 12, no. 2, pp. 2158–2173, Jan. 2025.
[14] H. Wang, C. Chen, Z. Zeng, S. Shao, and H. Haas, “Bidirectional retroreflective optical ISAC using time division duplexing and clipped OFDM,” *IEEE Photon. Technol. Lett.*, vol. 37, no. 10, pp. 587–590, May 2025.
[15] S. Chen, C. Chen, Z. Zeng, Y. Yang, and H. Haas, “Full-duplex RO-ISAC system: Wavelength division duplexing and hybrid waveForm design,” *IEEE Photon. Technol. Lett.*, vol. 37, no. 15, pp. 869–872, Aug. 2025.
[16] Y. Wang, C. Yang, Y. Wang, and N. Chi, “Gigabit polarization division multiplexing in visible light communication,” *Opt. Lett.*, vol. 39, no. 7, pp. 1823–1826, 2014.
[17] X. Xiong, H. Wang, S. Shao, and C. Chen, “Hybrid MRR-assisted long-range SDMA for RO-ISAC systems in industry IoT applications,” *J. Lightw. Technol.*, vol. 44, no. 5, pp. 1786–1799, 2026.